

## Whistler Evidence of Large-Scale Electron-Density Irregularities in the Plasmasphere

C. G. PARK AND D. L. CARPENTER

*Radioscience Laboratory, Stanford University  
Stanford, California 94305*

Large-scale structure in electron density in the plasmasphere has been identified from whistlers recorded at Eights, Antarctica, near sunspot minimum. The structures have dimensions of the order of an earth radius at the equator. Examples of the structures include an outlying peak in equatorial electron concentration near  $L = 4$ , with peak-to-valley ratio of 2, and more than 3:1 variations in electron concentration within  $30^\circ$  in longitude. Once formed, the structures may be observed for several hours or more. Detailed information on the occurrence of the irregularities is not yet available, but it is believed that they tend to develop under the influence of magnetospheric convection events. The convection events tend to accentuate departure from 'smoothness' that originally developed through the action of ionosphere-protonosphere coupling processes and possibly through a cycle of erosion and accretion of plasma at the plasmasphere boundary in the dusk sector.

### INTRODUCTION

Large-scale irregularities in electron density have been found within the plasmasphere. The irregularities, often clearly evident in equatorial profiles obtained from individual multipath whistlers, have not been identified in previous studies that employed averages over data from several days.

Examples of departures from smoothness in electron density within the plasmasphere are shown in Figures 1 and 2, which present whistler measurements of equatorial electron density as a function of geocentric distance in earth radii. Figure 1 depicts an outlying peak in the radial distribution of ionization near  $4 R_E$ . The data first show a decrease in density with distance from  $2.8$  to  $3.5 R_E$ , then an increase by a factor of  $\sim 2$  to a peak, and then a further decrease.

Figure 2 is a composite of many measurements over several hours and is intended to show the existence of three distinct electron-density levels within the  $\pm 15^\circ$  longitudinal viewing range of the whistler receiver at Eights, Antarctica. Details of Figures 1 and 2 will be discussed below.

The conditions of repeatability, the scale, and the apparent form of the irregularities suggest that magnetospheric convection [Axford, 1969] plays a major role in their formation.

Whistler research has shown that convection activity occurs well within the plasmasphere, and that it includes slow cross- $L$  drifts of the order of  $0.1 R_E/\text{hour}$  [Carpenter, 1966], enhanced cross- $L$  drifts of  $\sim 0.3\text{--}1.0 R_E/\text{hour}$  near midnight during substorms [Carpenter and Stone, 1967], and also large, substorm-associated sunward surges near the dusk meridian [Carpenter, 1970]. These drifts can be imagined to have a mixing effect on the magnetospheric thermal plasma, since, for a locally homogeneous  $\mathbf{E}$  field, the magnitude of plasma drift velocity  $\mathbf{v}$  at the equator varies with geocentric distance  $R$  as  $R^2$  in the hydromagnetic relation

$$\mathbf{v} = \mathbf{E} \times \mathbf{B}/B^2$$

The plan of this paper is to describe measurements of electron content in a magnetospheric tube of ionization during a cross- $L$  drift event. The measurements indicate that tube content remains approximately constant during a rapid inward displacement. Proceeding on the assumption of content preserving drifts, simple convective models are suggested as a means of developing irregular magnetospheric profiles. These suggestions are followed by some examples of irregular structure deduced from whistler data.

### MEASUREMENT OF ELECTRON CONTENT IN MAGNETOSPHERIC FLUX TUBES

*Electron content in radially drifting tubes of*

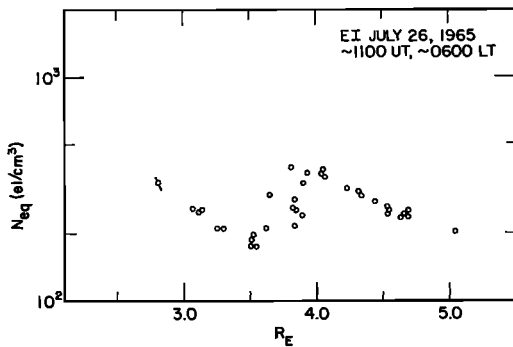


Fig. 1. Equatorial electron-density profile in the plasmasphere showing an outlying density peak near  $4 R_E$  geocentric distance. The profile was obtained from whistlers recorded at Eights, Antarctica. The short bar near  $2.8 R_E$  represents uncertainty due to measurement error associated with that point.

ionization. Tube electron content is defined as the total number of electrons above 1000 km altitude in a tube of magnetic flux with  $1 \text{ cm}^2$  cross-sectional area at 1000 km and extending to the geomagnetic equator. If a tube near  $L = 4$  undergoes a cross- $L$ , magnetic-flux-preserving drift through  $\Delta L \approx 1 R_E$ , then the bulk of the tube remains in the protonosphere. If particle fluxes through the ionospheric ends of the tube are sufficiently small, it can be expected that tube electron content will remain approximately constant during the motion, and that electron density will change roughly according to the change in volume of the tube. This section presents a set of measurements indicating conservation of tube content during a rapid, substorm-associated drift.

The values of electron tube content and equatorial density reported here were derived from whistler data through use of a diffusive-equilibrium model of the field-line distribution of ionization (adapted from Angerami [1966]). The parameters of the model are  $T_e = T_i = 1600^\circ\text{K}$  and, at the 1000-km reference level,  $n(\text{H}^+)/n_e = 8\%$ ,  $n(\text{O}^+)/n_e = 90\%$ , and  $n(\text{He}^+)/n_e = 2\%$ . The results are relatively insensitive to changes in these parameters. (For a review of the whistler method of measuring magnetospheric electron density and tube content, see Angerami [1966], Angerami and Carpenter [1966], or Carpenter and Smith [1964].) Dipole coordinates were used in the calcula-

tions, since relative changes are of primary interest, and since most of the results concern the magnetosphere at  $L < 5$  during planetary magnetic conditions ranging from quiet to only moderately disturbed.

The drift event (July 15, 1965, at 0615 UT) is summarized in Figure 3, which illustrates magnetic activity near  $L \sim 7$  (Byrd Station) and the measured dipole equatorial radius of two whistler paths as a function of time. The whistlers were recorded at Eights, Antarctica ( $L \sim 4$ , about 1 hour ahead of Byrd in geomagnetic time). Between 0614 and 0720 UT, the duct represented by triangles moved inward through  $\Delta L = 0.4 R_E$ , and the duct represented by circles through  $\Delta L = 3.35 R_E$ . (An  $R^{-3}$  scale is used for plotting equatorial distance, so that the slope of a curve will be proportional to the inferred east-west electric field at the magnetic equator, independent of  $R$ ; i.e., for a dipole field,  $d(R^{-3})/dt \propto E_\phi$ ). A previous report on this drift event was made by Carpenter and Stone [1967].

Figure 4a shows measured electron tube content versus equatorial radius for the two ducts whose radial drifts are shown in Figure 3. Solid symbols numbered 1, 2, and 3 identify measure-

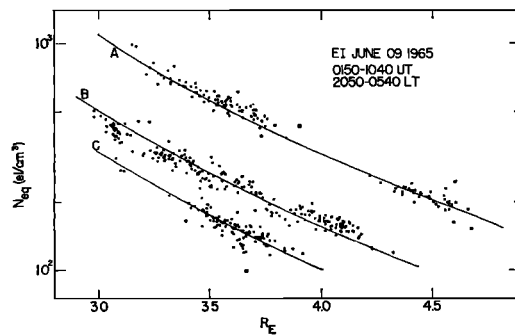


Fig. 2. Composite of a sequence of observations of equatorial electron density versus geocentric distance in the plasmasphere, showing the existence of three distinct density levels within the longitudinal viewing range of the whistler receiver at Eights, Antarctica. The individual observations were made several minutes apart and extended over a period of 9 hours. Curves A, B, and C were fitted on the assumption that, for each distinct group of data, electron content in a tube of ionization is constant with equatorial distance. A few of the points with values intermediate between the B and C levels are due to random measurement errors.

ments at three times: 0614 UT, just before the start of inward drift, and 0651 and 0720 UT, during later stages of the event. Open symbols represent intermediate times. It is evident that, for both ducts, measured electron tube content remained within a few per cent of a constant value while the ducts drifted inward.

The horizontal lines in Figure 4a represent arithmetic means of the sequence of measured values of tube content for each duct. The  $\sim 5\%$  scatter of data points about the means is attributed to measurement error. Uncertainties due to use of models of ionospheric density, temperature, and composition in the calculations principally affect absolute levels [Angerami, 1966], and within a given event might introduce small but relatively systematic errors of the order of 3%.

When a tube of ionization drifts inward, the end points move equatorward, and the cross-sectional area at 1000 km altitude increases. This effect was ignored in the present calculations, since the necessary correction is only about 1%. A similar effect involves the downward drift of tube end-points across a fixed altitude level.

For the kind of drift motions discussed in this paper, the error in tube content due to using a fixed base of 1000 km is only of the order of 1%. On the other hand, the vertical component of drift velocity may have significant effects on the ionosphere. This subject is now under study.

*Electron density during cross-L drifts of tubes of ionization.* A whistler-based measurement of the tube content also specifies a value of equatorial electron density, since a field-line model of magnetospheric plasma density is used in the tube-content calculation. There is then a one-to-one mapping between Figure 4a, showing measured tube content, and Figure 4b, showing corresponding values of equatorial electron density. The lines of constant content of 4a necessarily map to 4b as curves varying roughly inversely as the volume of the flux tubes, or as  $R^4$ . The points distributed along the two 'constant content curves' indicate density increases by a factor of  $\sim 1.5$  during the inward drifts through  $\Delta L \sim 0.4 R_E$ .

#### SIMPLE MODELS OF MAGNETOSPHERIC DENSITY IRREGULARITIES

From evidence in the preceding section, it is assumed that magnetospheric drifts preserve the electron content. A tentative means of interpreting whistler data of the kinds shown in Figures 1 and 2 is then as follows:

Even during magnetically quiet periods, electron tube content is not normally constant over the range  $2 < L < 6$ . Instead there is frequently an increase in content with increasing latitude, followed by a region of roughly constant content. Figure 5a shows an experimental profile of tube electron content versus tube equatorial radius, and Figure 5b shows the corresponding equatorial density profile, recorded under quiet nighttime conditions near sunspot minimum (from Angerami and Carpenter [1966]). Between  $L \sim 2.8$  and 3.8, the observed value of  $N_T$  rises by a factor of 3, and the corresponding equatorial profile behaves roughly as  $N = \text{constant}$ . Above  $L \sim 3.8$  the content is constant (over the region of measurement), and corresponding values of equatorial density fall off roughly as  $N_{eq} \propto R^{-4}$ . Localized increases in tube content with  $L$  of this type were observed frequently near sunspot minimum, and presumably are the result of factors such as the rapid increase in tube vol-

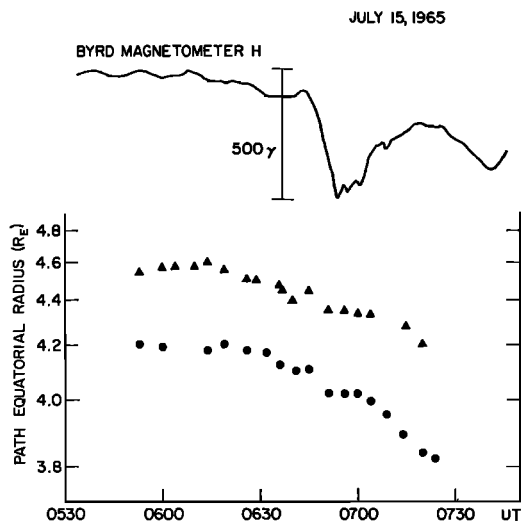


Fig. 3. Decrease in equatorial radius of two whistler ducts during a substorm [adapted from Carpenter and Stone, 1967]. The whistlers were recorded at Eights, Antarctica, near 0100–0200 LT. At the top is a transcription of the geomagnetic  $H$  component as observed at Byrd Station, Antarctica (about 1 hour behind Eights in magnetic time).

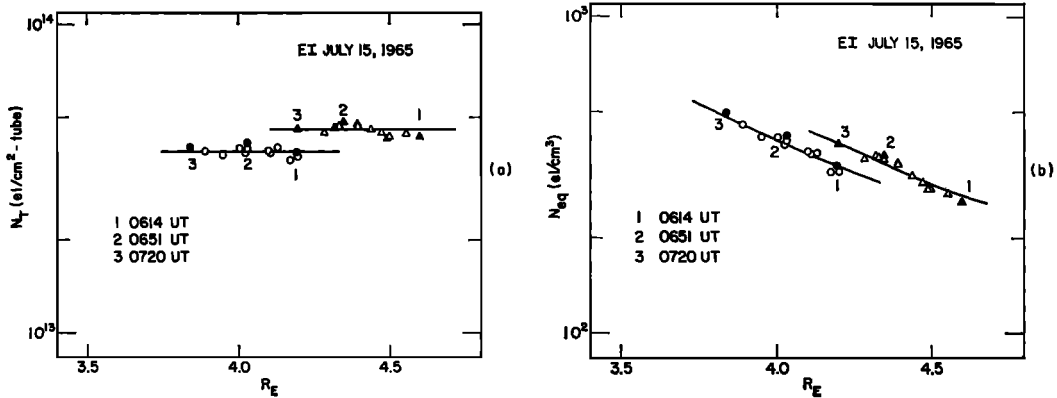


Fig. 4. (a) Tube electron content versus tube equatorial radius for the two ducts of Figure 3; the content remains approximately constant during inward drift (tube content is the total number of electrons in a tube of force with cross section  $1 \text{ cm}^2$  at  $1000 \text{ km}$  and extending from  $1000 \text{ km}$  altitude to the equator). Triangles and circles identify the ducts as in Figure 3. Measurements at times 1, 2, and 3 are represented by solid symbols; for intermediate times open symbols are used. The intermediate times were not always the same for the two ducts. Horizontal lines represent arithmetic means of  $N_T$  for each duct. (b) Equatorial electron density versus geocentric distance in earth radii, corresponding to the values of tube content in a.

ume with latitude, and latitudinal and temporal variations in protonospheric action as a reservoir or sink for ionospheric plasma [e.g., *daRosa and Smith, 1967*].

Much confusion has arisen over the relation between electron-density profiles transverse to and along the geomagnetic field. Cross- $L$  diffusion within the plasmasphere (at  $L > 2.5$ ) is clearly not fast enough to produce spherical symmetry in the plasma distribution; *Angerami and Carpenter [1966]* found evidence that the protonospheric field-line distribution of electrons follows a hydrostatic model, while the equatorial profile within the plasmasphere does not in general accord with such a model.

Perturbing substorm convection occurs in the presence of profiles such as the examples in Figure 5. The effect of the convection may be to 'amplify' pre-existing departures from smoothness in the profile and to change the orientation of density gradients. Some indication of the effect of radial substorm drifts is shown schematically in Figure 6, where both equatorial density (upper graph) and tube electron content (lower graph) are plotted as functions of tube equatorial radius. The density and content profiles are assumed to have the initial form of the solid curves, with

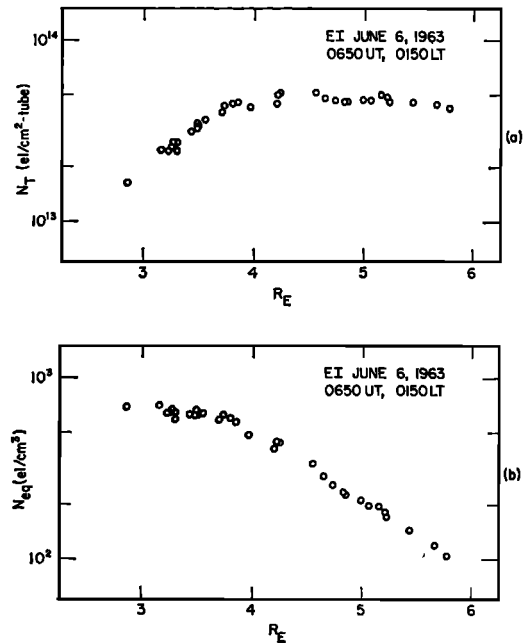


Fig. 5. (a) Profile of tube electron content (above  $1 \text{ cm}^2$  at  $1000 \text{ km}$ ) versus tube equatorial geocentric radius, deduced from a multipath nose whistler recorded at Eights, Antarctica, on a magnetically quiet night [adapted from *Angerami and Carpenter, 1966*]. (b) Equatorial profile of electron density corresponding to a.

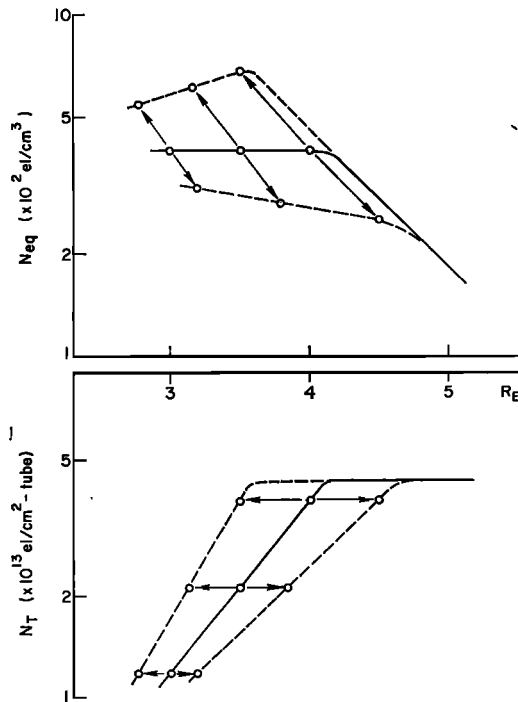


Fig. 6. Sketches suggesting the effects of radial (cross- $L$ ) drift events on the equatorial profile of electron density (top) and the tube content profile (bottom). The solid curves represent initial profiles; the upper and lower dashed curves represent conditions following assumed inward and outward content-preserving drifts, respectively.

constant density and hence increasing tube content between 3 and 4  $R_E$ , and density varying as  $N_{eq} \propto R^{-4}$  ( $N_T \sim \text{constant}$ ) beyond 4  $R_E$ . The upper and lower dashed curves show, respectively, the effects on the profiles of convection events involving westward and eastward electric fields of the order of 1 mv/m and 1–2 hours duration. This field  $E_\phi$  is assumed to be constant with  $R$ , so that convection velocity  $v_r$  varies as  $1/B$ . (One of the authors [Carpenter] has found empirical support for the relation  $v_r \propto 1/B$  in several substorm drift events wherein path radii were distributed over  $\Delta R \approx 1 R_E$ ). The drifts are assumed to preserve electron content, so that points representing particular flux tubes move along curves of constant content such as those illustrated in Figure 4. For inward drifts, the nonuniformity of displacement due to the variation of  $v_r$  with

$R$  leads to a more positive slope in those parts of the profiles that originally departed from the constant-content characteristic. In Figure 6, a peak in the equatorial profile develops at the 'bend' in the profile and moves progressively inward, increasing in scale with time. For outward drifts (lower dashed curves), the slope of the profiles becomes more negative in the regions of original departure from a constant-content characteristic. The tendency is then to attenuate the development of flattened segments or peaks in the equatorial distribution.

Figure 6 is an idealization, involving consideration of the effects of  $E_\phi$  only. For a potential field localized to some sector of the night-side magnetosphere,  $E_r$  must be important, and the longitudinal drifts accompanying the inward drifts must be considered in determining the actual behavior on a given meridian.

Other features of the development and modification of magnetospheric irregularities by means of convection are illustrated in Figures 7 and 8. Figure 7 shows the tendency for longitudinal gradients to develop under the influence of localized cross- $L$  drifts during substorms. (In a sense, the effect is shown in Figure 6, if it is

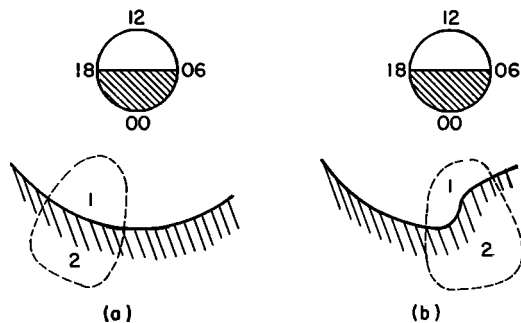


Fig. 7. Sketches suggesting how longitudinal gradients in electron tube content can develop through localized radial drifts acting in the presence of pronounced radial gradients. (a) Initially there are two regions with different tube content within the plasmasphere, a low-content region labeled 1 and a high-content region labeled 2. The dashed curve represents the equatorial viewing area of a whistler receiver near  $L = 4$  in the premidnight sector. (b) A substorm-associated convection event has occurred, involving cross- $L$  inward displacement of plasma on the midnight side of 2300 LT and the development of longitudinal gradients in electron tube content and density within the viewing area of the receiver.

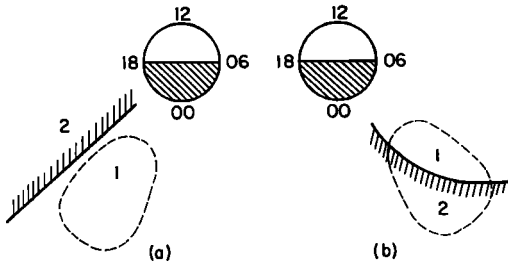


Fig. 8. Sketches suggesting how an outlying peak in the equatorial electron-density profile can develop through azimuthal drifts acting in the presence of longitudinal gradients in tube electron content. Dashed curves represent the equatorial viewing area of a whistler receiver near  $L = 4$ . (a) A low-content region labeled 1 and a high-content region labeled 2 are separated by a meridional 'boundary.' The whistler receiver 'sees' only the low-content region. (b) A convection event involving an assumed homogeneous electric field directed radially inward causes the plasma to overtake the ground receiver, but with larger angular velocity at greater distances, so that the receiver now sees low tube content at low  $L$  and high content at high  $L$ .

imagined that the substorm convection event giving rise to the upper dashed curve occurs in a localized region, leaving the solid curve to apply nearby.) In Figure 7a the existence of a radial gradient in tube electron content (such as that between 3 and 4  $R_E$  in Figure 6, lower graph) is indicated schematically by a line separating an inner low-content region (1) and an outer (hatched) high-content region (2). The estimated equatorial 'viewing' area of the ground receiver at Eights is shown by a dashed curve. The effect of a substorm convection event is shown schematically in Figure 7b. Enhanced inward motions of the plasma have occurred for  $\sim 1$  hour within a region restricted to the midnight side of the 2300 LT meridian (experimental evidence of this effect is considered below). The result is a warping of constant-content contours and the development of a significant longitudinal gradient of tube electron content.

Figure 8 illustrates a means of developing a peak in the radial density profile through non-uniform azimuthal drift (as compared to the nonuniform radial drift employed in Figure 6). A longitudinal gradient in tube content (or density) is identified by a line separating a hatched high-density region from a lower-density

one. In Figure 8a, the ground station is viewing an equatorial sector of the magnetosphere entirely within the 'low content' region. As time passes between 8a and 8b, convection associated with a substorm occurs such that, near the viewing area, the  $E$  field is large in scale and predominantly north-south (radially inward). The azimuthal drift  $v_p$  varies as  $1/B$  (if  $E_r$  is assumed to be independent of  $R$ ), and the boundary of the hatched region becomes spiral-shaped. The dense region tends to overtake the ground station, but differentially in  $R$  so that at the time of 8b the station 'sees' predominantly dense plasma at higher  $L$  and predominantly low-density plasma at low  $L$ .

#### DETAILS OF IRREGULAR ELECTRON-DENSITY STRUCTURE

*Radial gradients.* Figure 9 presents additional examples of the 'flattening' effect at lower  $L$  shells illustrated in Figure 5b. In both Figures 9a and b, the  $N \approx$  constant behavior extends to  $\sim 3.5 R_E$  and is followed by decreases roughly as  $N \propto R^{-4}$ . Again as in Figure 5, the planetary magnetic conditions were quiet, with maximum 3-hour  $Kp$  of 2<sub>-</sub> during the preceding 24 hours. To illustrate the variety of conditions that can occur, Figure 9c shows another profile for quiet conditions (max.  $Kp = 1_+$ ), this time with only a moderate decrease in slope within  $L \sim 3.8$ . Thus electron density at  $L \sim 3$  in Figure 9c is a factor of about 2 greater than in 9a, while the  $L \sim 4$  values agree within about 20%. Figures 9a and 9c are composites of data taken over periods of several hours. The relatively small amount of scatter in the data (and in 9b) implies a corresponding absence of large longitudinal variations within the viewing range of the receiver.

Figure 9d shows the outlying peak effect illustrated in Figure 1, but with less detail near the peak. For Figure 1, magnetic activity was low after a moderate disturbance, whereas for Figure 9d activity was moderate after quiet conditions. The scatter in Figure 1 on the low- $L$  side of the peak may be due to a variation in the  $L$  value of the peak with longitude.

*Longitudinal structure.* The complex, overlapping whistler spectra in Figure 10 (0-8 kHz versus time) indicate the presence of two distinctly different electron density 'levels' within the view of the whistler station at Byrd.

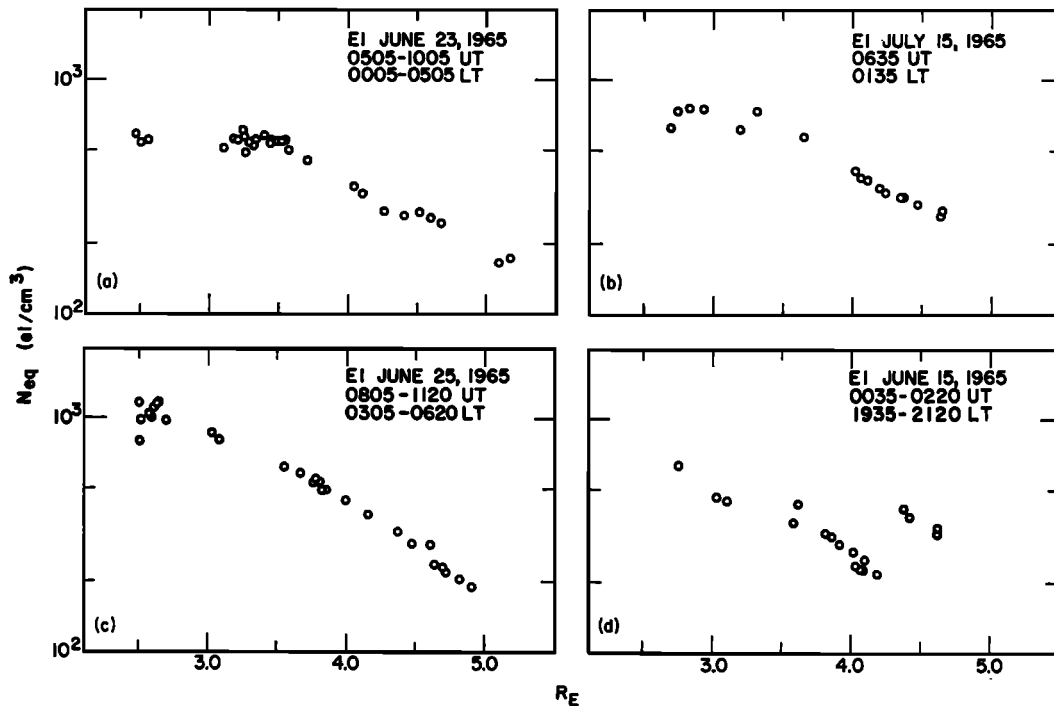


Fig. 9. Examples of 'irregular' behavior of equatorial electron-density profiles in the plasmasphere, deduced from whistlers recorded at Eights, Antarctica, near solar-cycle minimum: (a) and (b), 'flattening' of profiles at low  $L$  values; (c), a slight flattening tendency below  $L = 3.8$ ; (d) a profile with an outlying peak.

In the associated electron-density plot of Figure 11, the solid symbols represent the whistler in the top panel of Figure 10, and the open circles represent other whistlers recorded at  $\sim 1335$  UT and also at  $\sim 1235$  UT (synoptic, 2 min/hour observations). In Figure 10, the traces exhibiting a frequency of minimum travel time or nose frequency of 5–6 kHz and travel times near 1.5–1.6 sec represent the low-density regime; traces with similar nose frequency and travel times of 1.8–2.2 sec represent the higher-density level. The lack of scatter in data points within each group in Figure 11 suggests that the two density regimes are spaced in longitude, at least from  $L \sim 3.8$  to  $L \sim 4.3 R_E$ . This interpretation is reinforced by the spectra themselves. In the top and middle records a single lightning flash excites both high- and low-density paths, producing a pattern of overlapping traces. In the bottom record a lightning flash excites only the high-density, high-travel-time family of traces. This occa-

sional separate excitation of a particular density group indicates that the low and high densities are not part of an extremely irregular profile on a given meridian, but are actually displaced from one another in longitude.

*Time variations.* Figure 2 is a composite of electron-density observations over a 9-hour period, and suggests the presence of three relatively distinct plasmasphere density levels within the longitudinal viewing range of the Eights whistler station. This case appears to be a typical example of multi-level profiles, except that it has 3 levels instead of the more common 2.

The interval 0150–1040 UT (2050 to 0540 LT) represented in Figure 2 includes periods during which large cross- $L$  drifts associated with perturbing substorms are frequently observed in the plasmasphere [Carpenter and Stone, 1967, 1968; Carpenter *et al.*, 1969]. If the drifts are localized in the manner suggested in Figure 7, longitudinal gradients may tend to develop or

be enhanced. Some details of the cross- $L$  drifts of whistler paths during the June 9 observing periods are shown in Figure 12. At the top is a transcription of the magnetometer  $H$  component from Byrd Station (about 1 hour behind Eights in geomagnetic time). Below, in the manner of Figure 3, are plotted various whistler path radii observed at Eights. Broad arrows indicate that the local plasmopause radius was greater than  $4.7 R_E$  near 0000 LT and  $\approx 3.7 R_E$  near 0600 LT. The inward displacement from 0000 to 0600 LT is in rough agreement with motions observed inside the boundary.

Figure 12 illustrates a tendency for substorm-associated inward drifts to occur only after about 2300 LT at the observing station. Between about 2200 and 2300 LT, a period of moderate substorm activity at Byrd, two ducts move outward at a rate of roughly  $0.15 R_E$ /hour, corresponding to an eastward electric field component of  $\sim 0.15$  mv/m. At the same time ducts at larger  $L$  values do not show detectable radial drifts, a result that may be due to the distribution of whistler paths over longitude in the presence of spatial structure in the local convection activity. Between 2300 and 0100 LT there is quieting and no well defined cross- $L$  movement. Then, roughly 20 min before a large substorm bay at 0120 LT, inward drift begins at a rate of  $\sim 0.2 R_E$ /hour near  $L = 4$ , and at a slightly lower rate near  $L = 3.5$ . These rates correspond to a westward  $E$  field of  $\sim 0.2$  mv/m at  $L = 4$ , and  $\sim 0.13$  mv/m at  $L = 3.5$ . The drifts persist during protracted substorm activity until  $\sim 0400$  LT (the amplitude of the inward drift activity is somewhat less than that usually observed during substorms, whereas the duration of the drifts is somewhat longer than usual).

A history of observed tube content and electron density versus  $L$  for the event of June 9, 1965, is shown in Figure 13. Data for different times are not necessarily from the same set of ducts, and hence shifts in equatorial radius from panel to panel do not directly reflect the motions of the ducts. The solid lines are three constant-content curves obtained in the manner of Figure 4, except that several ducts were observed and tracked, and the constant-content curves were obtained by averaging within each density level over all the measurements shown

in Figure 2. The individual measurements of Figure 2 were typically spaced 2–3 min apart.

At 0322 UT (top of Figure 13), tube content increases with  $L$  value (upper left), and equatorial electron density (upper right) is approximately constant. There are three distinct levels of tube content, but the three groups of data points do not overlap in  $L$  at this time. The profiles for 0322 LT are representative of the period  $\sim 0250$  to  $\sim 0530$  UT. At 0550 UT (second row), near the beginning of inward drift, data groups  $B$  and  $C$  show overlap in  $L$ , and hence the profiles are double-valued. (Simultaneous whistler recordings at Byrd show whistlers belonging to the  $B$  group, but no whistlers belonging to the  $A$  or  $C$  groups. These recordings provides qualitative support for interpretation of the Eights data in terms of longitude separation of various duct groups.) At 0757 UT (third row), after further inward drift has taken place, all three groups overlap in  $L$ . Near  $L = 3.5$ , equatorial electron densities differ by a factor of 3.3 within the longitudinal view of the station. At 0949 UT (bottom row), group  $C$  has disappeared, and there is no overlapping between groups  $A$  and  $B$ .

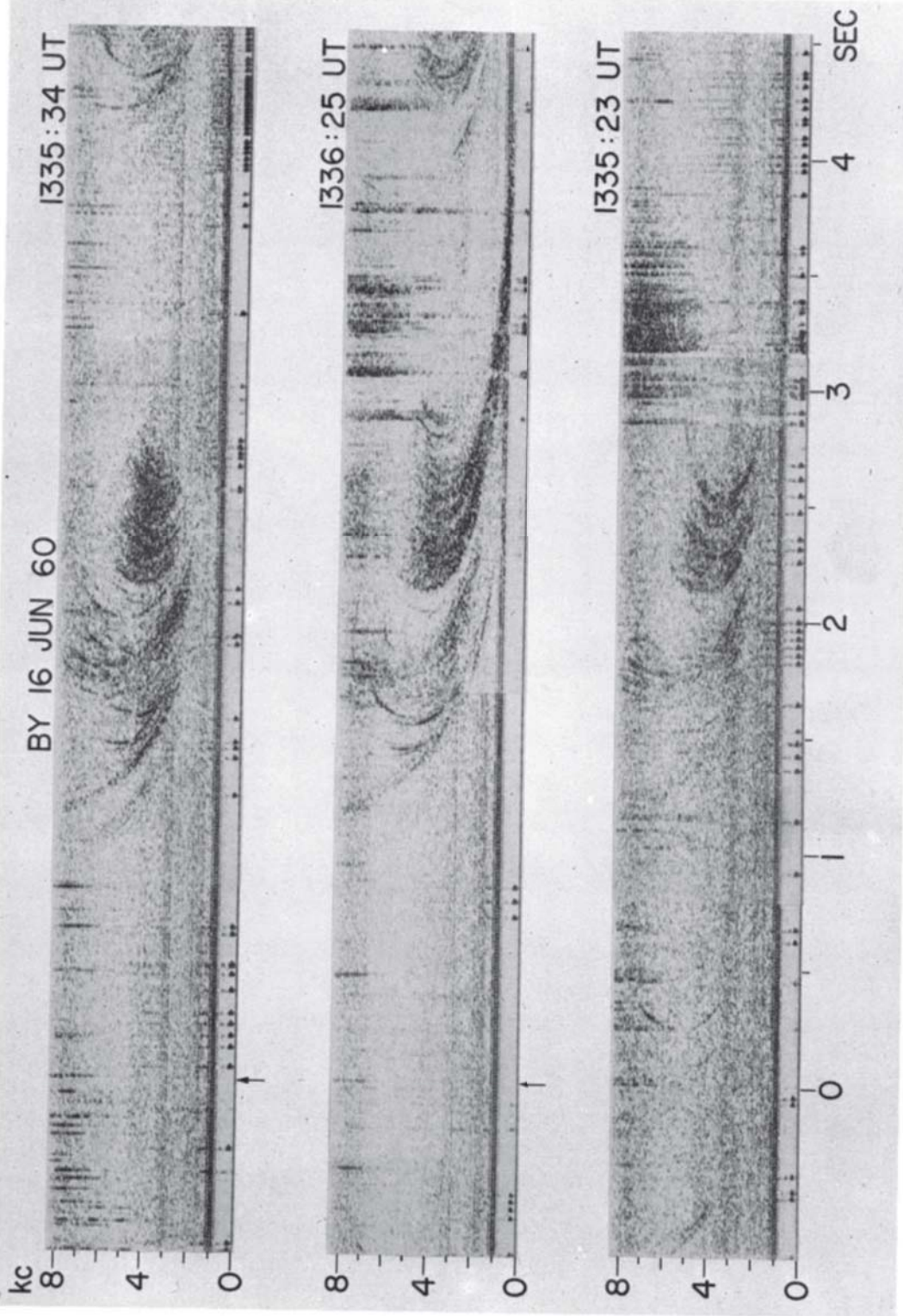
The data of Figures 2 and 13 suggest that at the beginning of the observations there were three distinct content sectors within the view of the station. As time passed, cross- $L$  (and azimuthal) drifts occurred. The sectors evidently moved so as to preserve their electron tube content, and there may have been shifting and warping of constant-content contours in the ways suggested in Figures 7 and 8. The tendency for nonuniform azimuthal drifts to occur is suggested by the disappearance of  $C$ -level densities from the 'view' of the station (Figure 13, bottom panels).

In Figure 2, the small number of density measurements at intermediate levels suggests that the regions of relatively high density gradient separating the density 'sectors' are narrow,

---

Fig. 10. (*Opposite*). Frequency-time whistler records from which the existence of longitudinal electron-density structure is inferred. The observing station in Byrd, Antarctica, at  $L \sim 7$ . Arrows and the origin of the time scale identify the causative atmospherics for the three whistlers in the center of the panels. Other whistlers appear at the upper and middle right and lower left.





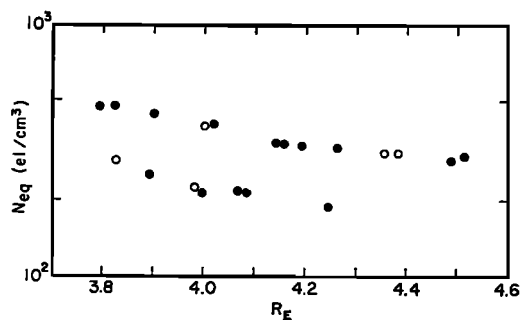


Fig. 11. Equatorial electron density versus geocentric distance, determined from the whistlers of Figure 10. Solid circles represent the whistler in the top panel of Figure 10, open circles represent other whistlers recorded at  $\sim 1335$  UT and also at  $\sim 1235$  UT (synoptic, 2-min/hour observations).

and hence have a low probability of being penetrated by the limited number of whistler paths that are active in a given period. Whistler ducts can evidently exist in regions of large longitudinal gradient, since cases have been found

in which two relatively distinct profile levels are connected by points at intermediate levels.

It should be possible to study some details of magnetospheric convection by identifying density sectors and then inferring changes in the sector topology from whistler measurements of the kind just described. From such measurements, particularly at stations spaced by about 20 degrees in longitude, it should be possible to estimate azimuthal as well as cross- $L$  drifts.

*Further remarks on irregular structure.* The frequency of occurrence of irregular density structure is not yet well known. It is known that when such structures develop they can last for many hours, sometimes for one or more days.

It is possible that some irregular structures originate in the dusk sector of the magnetosphere, where high-latitude convection appears to produce irregular longitudinal motions of the plasmasphere bulge [Carpenter, 1970] and also erosion of plasma during periods of enhanced convection [Taylor *et al.*, 1970; Chappell

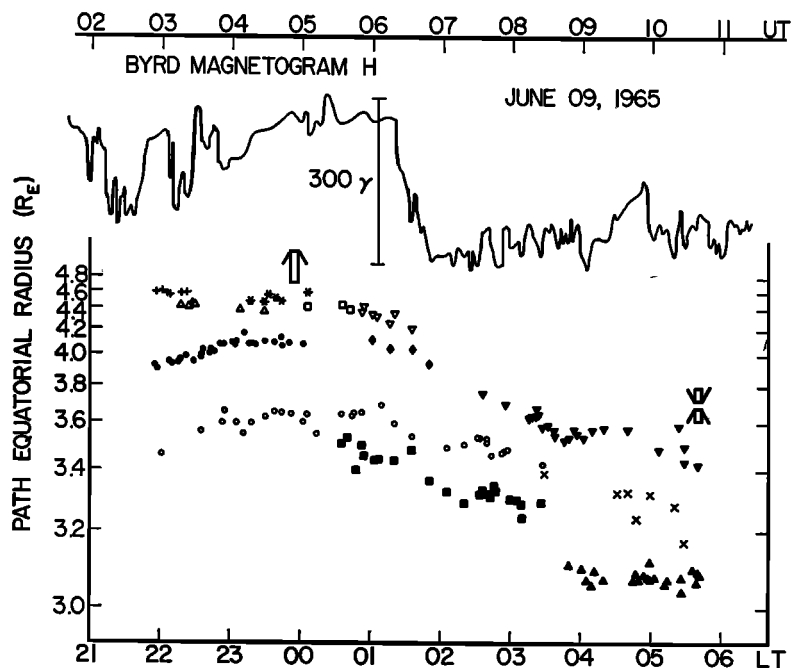


Fig. 12. An example of substorm-associated changes in whistler path equatorial radii during local nighttime, illustrating the local-time dependence of drift motions near midnight. Different symbols are used to represent different ducts. A transcription of the magnetogram from Byrd (about 1 hour behind Eights in magnetic time) is shown at the top. The broad arrow near local midnight indicates the inner limit of the plasmopause position. Two arrows near 0600 LT show that the plasmopause is between 3.6 and 3.8  $R_E$ .

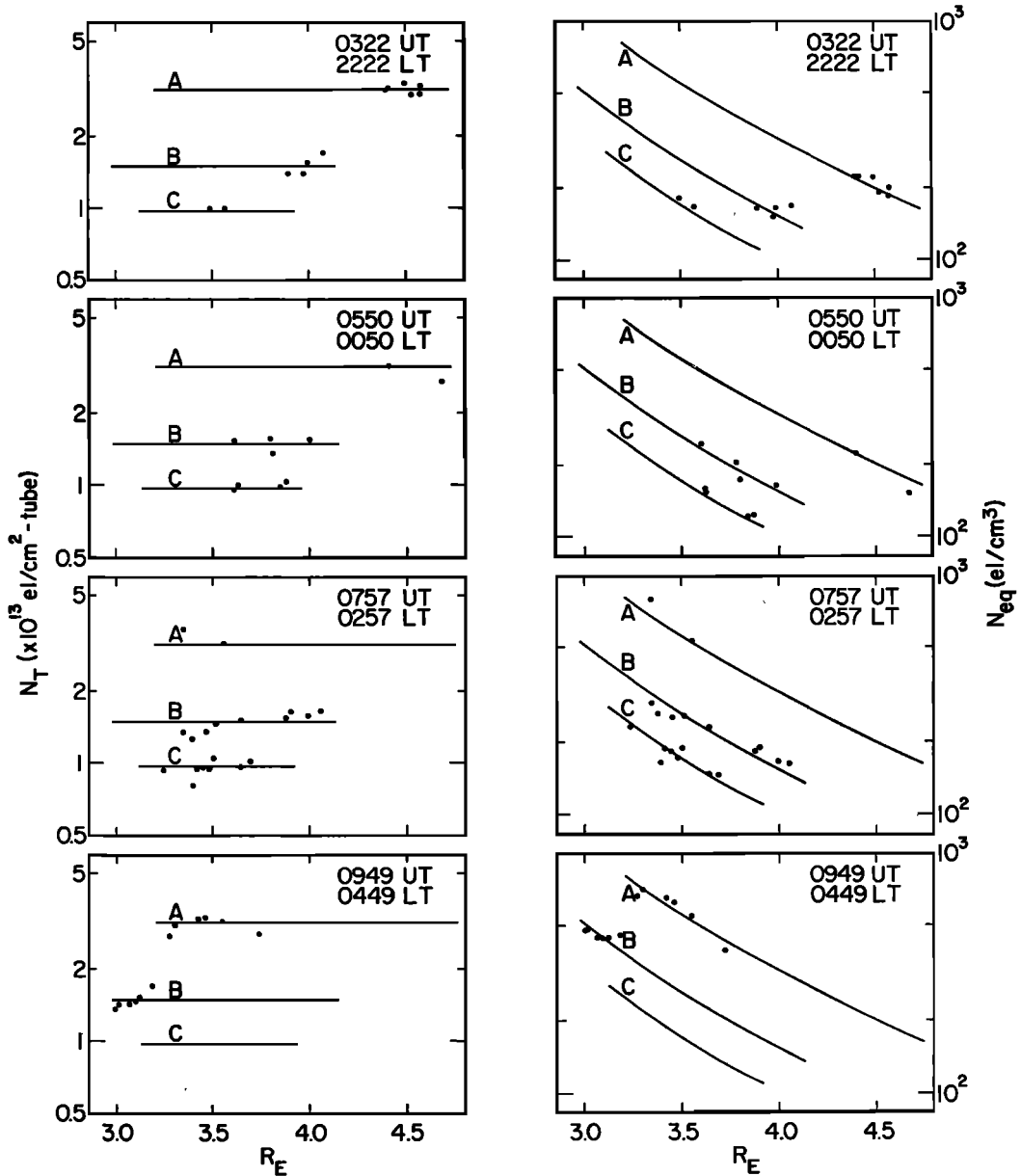


Fig. 13. A representative sequence of observations of electron tube content (left) and equatorial electron density (right) involved in the composite presentation of Figure 2. Equatorial density curves marked *A*, *B*, and *C* are the same as in Figure 2, and their corresponding tube contents are shown as horizontal lines on the left. During radial motion, the ducts moved approximately along the curves *A*, *B*, and *C*, maintaining their constant-content 'identity.' Points for different times are not necessarily from the same set of ducts, so that the apparent shifts in position of data points do not directly reflect the motions of the ducts.

*et al.*, 1970]. In the dusk sector, tubes of ionization whose equatorial electron densities vary over a wide range up to plasmaspheric levels (depending on a tube's individual convection history) may be involved in a cycle of capture by the plasmasphere and release therefrom as substorm activity wanes and then increases. This may produce a kind of density modulation in the outer part of the rotating plasmasphere. Such initial modulation may then be accentuated and otherwise altered by the convection processes discussed above.

Information on longitude variations in magnetospheric plasma density is provided by thermal-ion mass spectrometer measurements from eccentric orbiting satellites. As an example, OGO 1 measurements by *Taylor et al.* [1968] were made on June 9, 1965, the day of the whistler study reported above, but in a different longitude sector on the day side of the earth. Within the plasmasphere the satellite encountered a change in plasma density by a factor of about 3 within  $\Delta L \sim 0.2 R_E$ . Within this  $L$  interval the satellite moved through about 5 degrees in longitude, and it is inferred that the primary effect was longitudinal. The region of the plasmasphere crossed by OGO 1 was near the longitude of Kiruna during the preceding local night (assuming approximate co-rotation with the earth), and experienced a series of closely spaced substorms in much the same way that Eights experienced such activity a few hours later.

An unusual set of whistler observations during the IGY year of 1958 also provides qualitative support for the existence of longitudinal structure in the magnetosphere. A series of lightning flashes in the southern hemisphere produced simultaneous whistlers at the northern hemisphere stations Seattle and Unalaska, both at  $L \sim 3$  but separated by about 30 degrees in longitude. Each station observed whistler components in roughly the same  $L$  range, but travel times at Unalaska were systematically less than at Seattle, indicating a corresponding longitudinal difference in electron density by about a factor of 2.

#### CONCLUSIONS

Evidence has been found of irregular structure in magnetospheric electron density. In radial profiles at the magnetic equator, the

irregularities frequently take the form of 'flattening' effects, wherein the electron density at  $\sim 2.5 < L < 4$  may be constant or show regions of increase with distance. Outlying increases in density with peak values a factor of 2 greater than the minimum value within have been observed. Evidence of large longitudinal gradients has been found; in the example discussed, electron density varied by a factor of 3 at a given  $L$  value within roughly 30 degrees longitude. It is inferred that on this occasion there were relatively large sectors of relatively constant electron tube content separated by relatively narrow regions of large density gradient.

It is believed that the irregularities develop through a combination of magnetospheric convection events and ionosphere-protonosphere coupling processes. A kind of density modulation of the outer plasmasphere may occur through irregular substorm-associated convection and the associated erosion-accretion processes that apparently occur at the plasmasphere bulge in the dusk sector. Ionosphere-protonosphere coupling processes can apparently give rise to localized depletions or 'flattening' effects in the equatorial electron-density profile at  $L \lesssim 3.5$ . Convection events within the plasmasphere may then enhance or otherwise modify the initial departures from smoothness. In particular, the localization of cross- $L$  drifts may cause relatively large longitudinal gradients to develop. Irregular structures may sometimes be observed for many hours and may thus serve as tracers of plasma motions.

*Note added in proof.* Density variations with longitude outside the plasmapause have been reported by K. Bullough and J. L. Sagredo in the article 'Longitudinal structure in the plasmapause: VLF goniometer observations of knee-whistlers,' *Nature*, 225, 1038-1039, March 14, 1970.

*Acknowledgments.* This research was supported in part by the Office of Antarctic Programs of the National Science Foundation under grants GA-1151 and GA-1485 and in part by the Atmospheric Sciences Section of the National Science Foundation under grants GA-775 and GA-10719.

The Editor wishes to thank Dr. N. M. Brice and Dr. M. J. Rycroft for their assistance in evaluating this paper.

## REFERENCES

- Angerami, J. J., A whistler study of the distribution of thermal electrons in the magnetosphere, PhD Thesis, *Rep. SEL-66-017*, Radioscience Laboratory, Stanford Electronics Labs., Stanford University, 1966.
- Angerami, J. J., and D. L. Carpenter, Whistler studies of the plasmopause in the magnetosphere, 2, Equatorial density and total tube electron content near the knee in magnetospheric ionization, *J. Geophys. Res.*, **71**, 711, 1966.
- Axford, W. I., Magnetospheric convection, *Rev. Geophys.*, **7**, 421, 1969.
- Carpenter, D. L., Whistler studies of the plasmopause in the magnetosphere, 1, Temporal variations in the position of the knee and some evidence on plasma motions near the knee, *J. Geophys. Res.*, **71**, 693, 1966.
- Carpenter, D. L., Whistler evidence of the dynamic behavior of the dusk-side bulge in the plasmasphere, *J. Geophys. Res.*, **75**(19), 1970.
- Carpenter, D. L., and R. L. Smith, Whistler measurements of electron density in the magnetosphere, *Rev. Geophys.*, **2**, 415, 1964.
- Carpenter, D. L., and K. Stone, Direct detection by a whistler method of the magnetospheric electric field associated with a polar substorm, *Planet. Space Sci.*, **15**, 395, 1967.
- Carpenter, D. L., and K. Stone, Recent whistler research on hydromagnetic motions in the plasmasphere, paper presented at International Symposium on the Physics of the Magnetosphere, Washington, D. C., Sept. 1968.
- Carpenter, D. L., K. Stone, and S. Lasch, A case of artificial triggering of VLF magnetospheric noise during the drift of a whistler duct across magnetic shells, *J. Geophys. Res.*, **74**, 1848, 1969.
- Chappell, C. R., K. K. Harris, and G. W. Sharp, The morphology of the bulge region of the plasmasphere, *J. Geophys. Res.*, **75**(19), 1970.
- daRosa, A. V., and F. L. Smith, III, Behavior of the nighttime ionosphere, *J. Geophys. Res.*, **72**, 1829, 1967.
- Taylor, H. A., H. C. Brinton, and A. R. Deshmukh, Observations of irregular structure in thermal ion distributions in the duskside magnetosphere, *J. Geophys. Res.*, **75**(13), 1970.
- Taylor, H. A., Jr., H. C. Brinton, and M. W. Pharo, III, Contraction of the plasmasphere during geomagnetically disturbed periods, *J. Geophys. Res.*, **73**, 961, 1968.

(Received November 24, 1969;  
revised March 5, 1970.)